

Optical spectroscopy and the UV luminosity function of galaxies in the Abell 1367, Coma and Virgo clusters.*

L.Cortese¹, G.Gavazzi¹, J.Iglesias-Paramo², A.Boselli² and L.Carrasco^{3,4}

¹ Università degli Studi di Milano-Bicocca, P.zza della Scienza 3, 20126 Milano, Italy.

e-mail: Luca.Cortese@mib.infn.it; Giuseppe.Gavazzi@mib.infn.it

² Laboratoire d'Astrophysique de Marseille, BP8, Traverse du Siphon, F-13376 Marseille, France.

e-mail: jorge.iglesias@oamp.fr; alessandro.boselli@oamp.fr

³ Instituto Nacional de Astrofísica, Óptica y Electrónica, Apartado Postal 51 C.P. 72000 Puebla, Pue., Mexico.

e-mail: carrasco@transum.inaoep.mx

⁴ Observatorio Astronómico Nacional/UNAM, Ensenada B.C., Mexico.

Received 12 November 2002; accepted 14 January 2003

Abstract. Optical spectroscopy of 93 galaxies, 60 projected in the direction of Abell 1367, 21 onto the Coma cluster and 12 on Virgo, is reported. The targets were selected either because they were detected in previous $H\alpha$, UV or r' surveys. The present observations bring to 100% the redshift completeness of $H\alpha$ selected galaxies in the Coma region and to 75% in Abell 1367. All observed galaxies except one show $H\alpha$ emission and belong to the clusters. This confirms previous determinations of the $H\alpha$ luminosity function of the two clusters that were based on the assumption that all $H\alpha$ detected galaxies were cluster members. Using the newly obtained data we re-determine the UV luminosity function of Coma and we compute for the first time the UV luminosity function of A1367. Their faint end slopes remain uncertain ($-2.00 < \alpha < -1.35$) due to insufficient knowledge of the background counts. If 90% of the UV selected galaxies without redshift will be found in the background (as our survey indicates), the slope of UV luminosity function will be $\alpha \sim -1.35$, in agreement with the UV luminosity function of the field (Sullivan et al. 2000) and with the $H\alpha$ luminosity functions of the two clusters (Iglesias-Paramo et al. 2002). We discover a point like $H\alpha$ source in the Virgo cluster, associated with the giant galaxy VCC873, possibly an extragalactic HII region similar to the one recently observed in Virgo by Gerhard et al. (2002).

Key words. galaxies: redshift; galaxies: luminosity function; galaxies: clusters: individual: Abell 1367, Coma, Virgo

1. Introduction

Multi-wavelength determinations of the luminosity function of galaxies belonging to nearby rich clusters are fundamental tools for shedding light on the process of galaxy evolution and, in conjunction with similar determinations of "field" galaxies, should help unveiling the role of the environment on galaxy evolution.

These determinations suffer from insufficient redshift coverage, a crucial parameter for discriminating the (minority of) cluster members from the background interlopers.

Luminosity functions based on narrow band (i.e. $H\alpha$) surveys are less affected by the redshift incompleteness: only emission-line galaxies in a narrow recessional veloc-

ity range are detected by the limited band-width of the adopted filters. Complementary redshift information is nevertheless highly recommended in order to reject background objects whose $H\beta$ or [OIII] lines would fall into the band designed for containing the redshifted $H\alpha$ line. Iglesias-Paramo et al. (2002) carried out a deep $H\alpha$ imaging survey of 1×1 degree area in Coma and A1367 clusters and obtained the first $H\alpha$ luminosity function of nearby clusters of galaxies. By that time approximately fifty percent of $H\alpha$ emitting galaxies had no estimate of the recessional velocity. With the aim of measuring the remaining redshifts and for confirming the $H\alpha$ emission of these galaxies we carried out the spectroscopic survey presented in this paper. As a side product we also obtained redshifts of several UV selected galaxies in Coma and A1367 regions which enable us to re-compute the UV luminosity functions of the two clusters.

The present paper is arranged as follows: Section 2 contains a description of the galaxy selection criteria. The observations and the data-reduction procedures are de-

Send offprint requests to: G.Gavazzi

* Based on observations obtained with the Loiano telescope belonging to the University of Bologna (Italy), with the G.Haro telescope of the INAOE (Mexico) and with the Calar Alto observatory operated by the Centro Astronómico Hispano Alemán (Spain).

scribed in Section 3. The new redshift are presented in Section 4 along with the data on one interesting object in the Virgo cluster. The $H\alpha$ and UV luminosity functions of A1367 and Coma are discussed in Section 5. Conclusions are briefly summarized in Section 6.

2. The sample selection criteria

Galaxies in the present study were primarily selected among objects, projected in the direction of the Abell 1367 and Coma clusters, with $H\alpha$ emission detected in the INT $H\alpha$ survey of (Iglesias-Paramo et al. (2002)) or selected from the r' survey by Iglesias-Paramo et al. (2003). The $H\alpha$ selected galaxies in the Coma cluster were all spectroscopically measured, while only 75% of them were observed in A1367. The r' selected galaxies with $r' \leq 17$ have been observed with a completeness of 64% and 92% for A1367 and Coma respectively.

In addition to these, we selected 20 targets with UV magnitude $m_{\text{uv}} < 18.5$ detected by the FOCA balloon-borne wide field UV camera ($\lambda = 2000\text{\AA}$; $\Delta\lambda = 150\text{\AA}$) (Donas et al. 1995 and Donas, private communication). The UV magnitude is defined as: $m_{\text{uv}} = -2.5\log(F_{2000}) - 21.175$, where F_{2000} is the flux in units of $\text{erg cm}^{-2} \text{s}^{-1} \text{\AA}^{-1}$. The spatial resolution of the UV data is 20 arcsec FWHM (Milliard et al. 1992). The astrometric accuracy of these data is therefore typically 3-5 arcsec, insufficient for unambiguously identifying spectroscopic targets and discriminating between stars and galaxies. To overcome this limitation, we cross-correlated the FOCA catalogues of A1367 and Coma with the r' band catalogue of galaxies ($r' < 21$) by Iglesias-Paramo et al. (2003), using a matching radius of 20 arcsec. In cases of multiple identifications we select the galaxy closest to the UV position. Including the present observations, spectra are available for 64% and 56% of the UV selected galaxies with an optical counterpart in A1367 and Coma respectively.

A dozen of faint $H\alpha$ emitting galaxies in the Virgo cluster with no estimate of the recessional velocity in the literature were also selected as filler objects. These were serendipitously found around bright VCC galaxies by visual inspection to the net ($H\alpha + N[II]$) frames obtained at the INT by Boselli et al. (2002).

3. Observations and data reduction

Long-slit, low dispersion spectra of 93 galaxies were obtained in several observing runs since 2001 using the imaging spectrograph BFOSC attached to the Cassini 1.5m telescope at Loiano (Italy), LFOSC at the 2.1m telescope of the Guillermo Haro Observatory at Cananea (Mexico), and with CAFOS attached to the 2.2m telescope of the Calar Alto Observatory (Spain). Table 1 lists the characteristics of the instrumentation in the adopted set-up.

The observations at Loiano (44 galaxies) were performed using a 2.0 or 2.5 arcsec slit, depending on the seeing

conditions, generally oriented E-W. The wavelength calibration was secured with exposures of HeAr lamps. The on-target exposure time ranged between 15 and 30 min according to the brightness of the targets.

The observations at Cananea (40 galaxies) were carried out with a 1.9 arcsec slit, generally oriented N-S. The wavelength calibration was secured with exposures of XeNe lamps. The on-target exposure time ranged between 20 and 40 min according to the brightness of the targets. The observations at Calar Alto (9 galaxies) were carried out with a 1.5 arcsec slit, generally oriented N-S. The wavelength calibration was secured with exposures of CdHe lamps. The on-target exposure time ranged between 15 and 30 min according to the brightness of the targets. In all runs the observations were obtained in nearly photometric conditions, with thin cirrus. The orientation of the slit was modified from the set-up given above when two adjacent objects could be observed in the same exposure. The data reduction was performed in the IRAF environment. After bias subtraction, when 3 or more frames of the same target were obtained, these were combined (after spatial alignment) using a median filter to help cosmic rays removal. Otherwise the cosmic rays were removed using the task COSMICRAYS and/or under visual inspection. The lamps wavelength calibration was checked against known sky lines. These were found within $\sim 1 \text{\AA}$ from their nominal position, providing an estimate of the systematic uncertainty on the derived velocity of $\sim 50 \text{ km s}^{-1}$. After subtraction of sky background, one-dimensional spectra were extracted from the frames. The redshift were obtained using the cross-correlation technique of Tonry & Davis (1979). This method is based on a "comparison" between the spectrum of a galaxy (or a star) whose redshift is to be determined, and a fiducial spectral template of a galaxy of appropriate spectral type to contain the wanted absorption/emission lines. The basic assumption behind this method is that the spectrum of a galaxy is well approximated by the spectrum of its stars, modified by the effects of the stellar motion inside the galaxy and by the systemic redshift. For this purpose high signal-to-noise spectra were taken of two template galaxies: VCC0066 (emission lines) and NGC221 (absorption lines), which were converted to the rest frame λ . The derived redshift are not transformed to Heliocentric.

4. Results

The velocity measurements obtained in this work are listed in Table 2 as follow:

Column 1: Galaxy designation. For Virgo cluster we use the VCC (Binggeli et al. 1985) and VPC (Young & Currie 1998) designations when available.

Column 2, 3: (J2000) celestial coordinates, measured with few arcsec uncertainty.

Column 4: r' band magnitude.

Column 5, 6: observed recessional velocity with uncertainty derived in this work. The latter quantity includes only statistical errors. The global uncertainty can be de-

Table 1. The spectrograph characteristics

Observatory	Spectrograph	Dispersion Å/mm	Coverage Å	CCD	pix μm
Loiano	BFOSC	198	3600 – 8900	1340 × 1300	EEV 20
Cananea	LFOSC	228	4000 – 7100	576 × 384	TH 23
Calar Alto	CAFOS	187	3600 – 10200	2048 × 2048	SIT 24

rived by adding in quadrature 50 km s^{-1} due to the uncertainty in the absolute wavelength calibration.

Column 7: type of lines (A=absorption; E=Emission)

Column 8: telescope (LOI=Loiano; CAN=Cananea, CAL=Calar Alto)

Column 9: galaxies selection band (UV, $H\alpha$ or r')

4.1. The Virgo cluster

Twelve redshift measurements presented in this work are of faint ($r' \leq 18$) objects in the Virgo cluster which were serendipitously detected near bright VCC galaxies as part of an $H\alpha$ imaging survey of this cluster (Boselli et al. 2002). Four of these galaxies turned out to be background galaxies whose emission, revealed in the net ($H\alpha + N[II]$) frames, is in fact due to $H\beta$ and $[OIII]$ lines, showing that at the faint limit of the survey the contamination by this type of objects becomes relevant.

We would like to draw the attention on the point-like $H\alpha$ source $122603+130724$ detected at the projected distance of $2'$ from the giant galaxy VCC873 shown in Fig. 1. The source shows an $H\alpha$ equivalent width of $\sim 700\text{\AA}$ and an $H\alpha$ flux $\sim 10^{-14.6} \text{ erg s}^{-1} \text{ cm}^{-2}$. In spite of its very faint continuum ($r' \sim 21.5$), the 15 min spectrum of this object taken with the Loiano 1.5m telescope yielded a prominent $H\alpha$ emission at 260 km s^{-1} , consistent with the velocity of VCC873 (232 km s^{-1}).

Unlike planetary nebulae (ICPNe) found near giant galaxies in the Virgo and Fornax cluster (Arnaboldi et al. 1996; Theuns & Warren 1997) showing strong $[OIII] \lambda 5007\text{\AA}$ lines (Dopita et al. 1992), $122603+130724$ is not detected in $[OIII]$. However, given the weakness of the available spectrum, the upper limit on $[OIII]$ is ~ 0.3 of the $H\alpha$ flux, therefore consistent with $122603+130724$ being an extragalactic HII region (Dopita et al. 2000) associated with the giant galaxy VCC873. The point-like $H\alpha$ source $122544+130740$ listed in Table 2 could be another extragalactic HII region, in this case not associated with a bright cluster galaxy. However the redshift of this faint ($r' \sim 20$) object, based on one line (presumably $H\alpha$) needs confirmation because it lies at a projected distance of 10 arcsec from a bright star.

Gerhard et al. (2002) found 17 candidate extragalactic HII regions in the Virgo cluster, among which the one associated with VCC836 was confirmed spectroscopically. Objects of this kind could account for the diffuse intra-cluster light (Bernstein et al. 1995) and might contribute

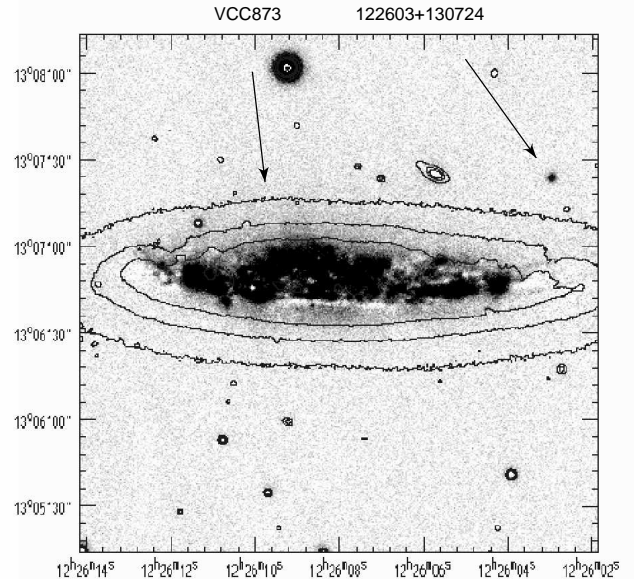


Fig. 1. Net $H\alpha+[NII]$ image of $122603+130724$ and VCC873 (grey-scale) with superposed contours of the continuum emission.

to the enrichment of the intergalactic medium in clusters.

5. The luminosity functions

5.1. The $H\alpha$ luminosity function

With the new data presented in this work, the redshift of all $H\alpha$ selected galaxies in the Coma cluster (Iglesias-Paramo et al. (2002)) have been measured. All objects turned out to be cluster members ($4000 < V < 10000 \text{ km s}^{-1}$) and significant $H\alpha$ emission was detected in their spectra. The $H\alpha$ luminosity function determined by Iglesias-Paramo et al. (2002) assuming that all objects were at the distance of Coma is fully confirmed.

In A1367 we measured the redshift of 14 galaxies, bringing to 75% the completeness of $H\alpha$ selected galaxies in this cluster. The membership to the cluster was confirmed for 13 galaxies, while 1 ($114430+195718$) turned out to be a background galaxy whose emission, revealed

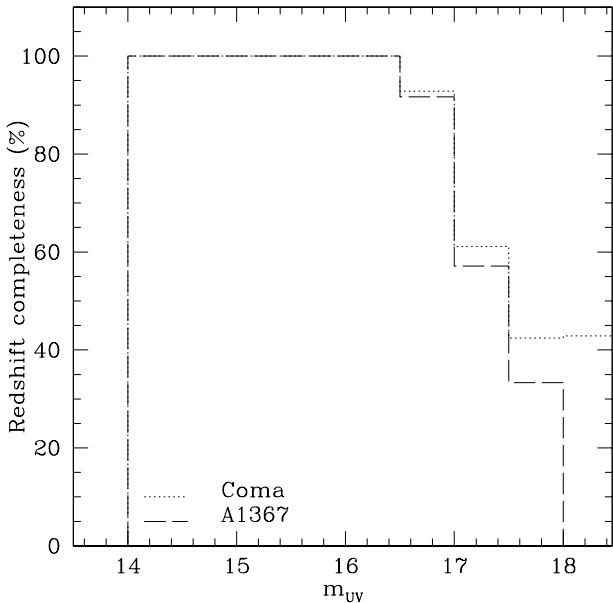


Fig. 2. Redshift completeness of the UV selected galaxies in Coma (dotted histogram) and A1367 (long dashed histogram). The redshift completeness is $\sim 90\%$ for $m_{UV} \leq 16.75$ while at fainter magnitudes it drops rapidly under 50%

by Iglesias-Paramo et al. (2002) is in fact due to $H\beta$ and [OIII] lines. This confirms that the $H\alpha$ survey by Iglesias-Paramo et al. (2002) is little contaminated by $H\beta$ and [OIII] emission lines from background objects, emphasizing the high success-rate of selecting emission line members with the Iglesias-Paramo et al. (2002) method.

5.2. The UV luminosity function

The $H\alpha$ luminosity functions of Coma and A1367 are found consistent one another, being characterized by a faint end slope $\alpha \sim -0.7$. This value differs significantly from the slope of the UV luminosity function of Coma (Andreon 1999, hereafter A99) $\alpha \sim -2.0$, the only UV luminosity function ever determined for a cluster. While stars with masses $M > 10M_{\odot}$ and lifetimes < 20 Myr contribute significantly to the $H\alpha$ flux, the UV emission is dominated by young stars of intermediate masses ($2 < M < 5 M_{\odot}$). Furthermore UV emission is detected also from early-type galaxies with no recent star formation episodes (Deharveng et al. 2002). However these differences alone are insufficient for producing discrepant luminosity function such as obtained in the two bands. Thus we use the spectroscopic observations presented in this work to re-compute the Coma UV luminosity function and to compute, for the first time, the UV luminosity function of A1367. Using the same UV data available to A99, we cross-correlate the UV detections with the r' catalogue of Iglesias-Paramo et al. (2003) for a better star/galaxy discrimination. This reduces our luminosity function determination to an area of $0.97^{\circ 2}$ (the

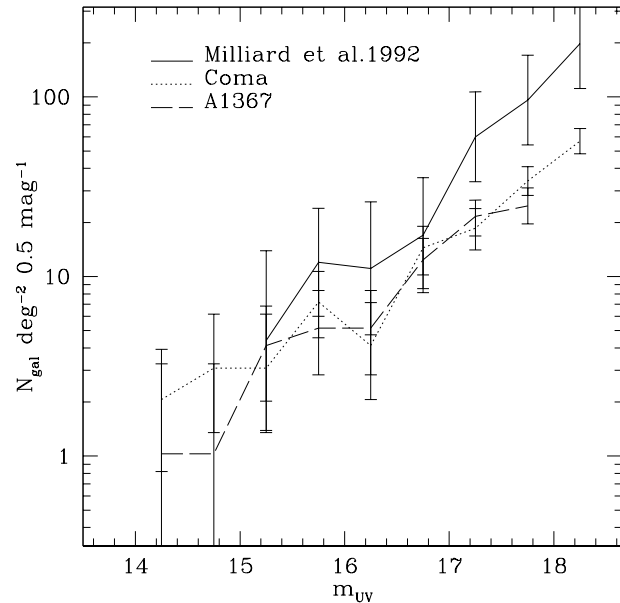


Fig. 3. Differential UV galaxy counts in the field by Milliard et al. 1992 (solid line), in the Coma (dotted line) and A1367 (long dashed line) clusters.

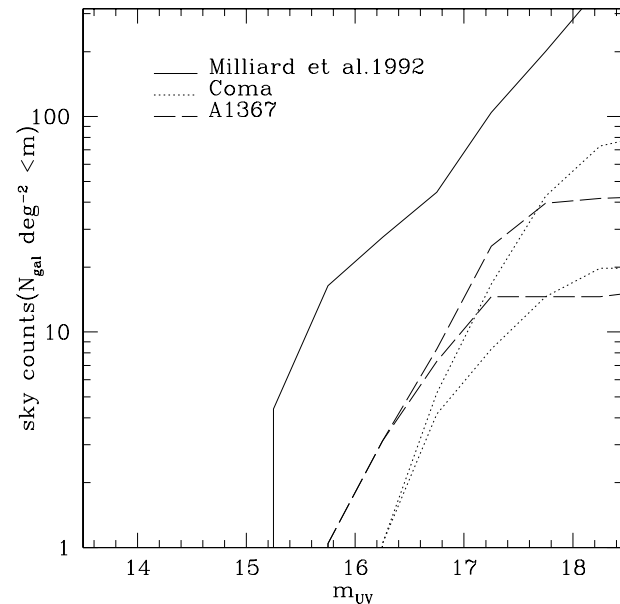


Fig. 4. Integrated UV galaxy counts in the field by Milliard et al. 1992 (solid line), upper and lower background limits for Coma (dotted line) and for A1367 (long dashed line) are given.

same over which we determined the $H\alpha$ luminosity function), instead of $\sim 3^{\circ 2}$ analyzed by A99. The determination of the cluster luminosity function requires a reliable estimate of the contribution of background/foreground objects to the UV counts. This can be accurately achieved for $m_{UV} \leq 16.75$, since for these UV sources the redshift completeness is $\sim 90\%$ (see Fig.2). At fainter mag-

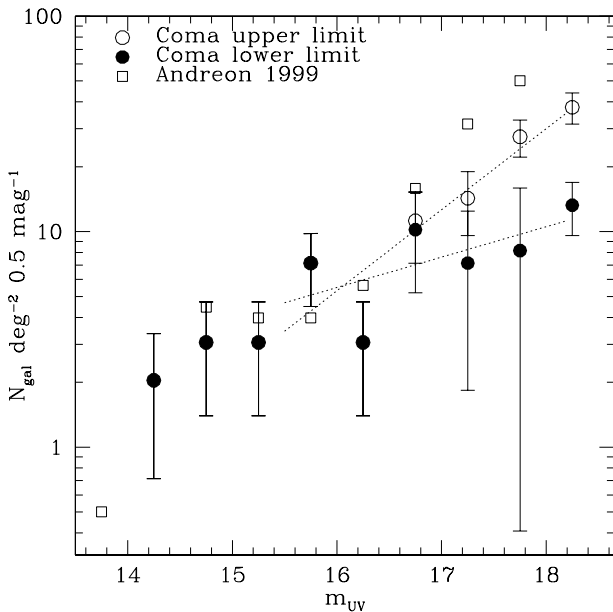


Fig. 5. The UV luminosity functions of the Coma galaxies. The luminosity function by A99 is represented with empty squares and the upper (empty circles) and lower (filled points) limits determined in this work are given. The dotted lines represent the best linear fits to the faint end of the luminosity function. Error bars account for Poissonian fluctuations.

nitudes the redshift completeness drops rapidly, thus requiring the contamination to be estimated statistically from the number of field galaxies, per bin of UV magnitude, that are expected to be randomly projected onto the cluster area. The over-density of UV counts due to Coma/A1367 galaxies can be derived from the difference between the counts in the direction of the two clusters and the UV galaxy counts derived in three random fields by Milliard et al. (1992) using the same experimental set up as for Coma and A1367. Opposite to our expectation the cluster galaxy counts at faint magnitudes are ~ 3 times lower than the Milliard et al. (1992) number counts (see Fig. 3), as already noticed by A99. The reason for such discrepancy is not fully understood and might reflect a higher degree of star contamination among the UV counts than estimated by Milliard et al. (1992). Alternatively it might derive from a higher than expected fraction of foreground galaxies in Milliard et al. (1992). However foreground galaxies should contribute significantly less than background objects due to the small sampled volume at $V < 4000 \text{ km s}^{-1}$. Using our new redshifts we can at least estimate a minimum and a maximum background contribution to the observed counts in the direction of Coma and A1367, a method followed by A99. The true background is at least composed of all objects whose velocity falls outside the assumed range for the clusters ($4000 < V < 10000 \text{ km s}^{-1}$). At most it comprises also all galaxies with unknown redshift. These limiting estimates,

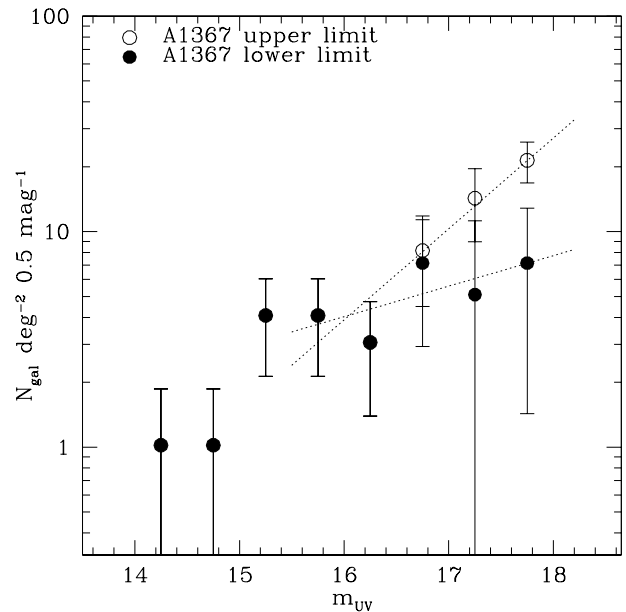


Fig. 6. Same as Fig. 5 for A1367.

shown in Figure 4 for Coma (dotted line) and A1367 (long dashed line), are found in good reciprocal agreement, but are significantly lower than the background counts estimated by Milliard et al. (1992). The resulting clusters UV luminosity functions should lie in between the two determinations given in Figs. 5 and 6.

Due to the large uncertainties we did not attempt to fit a complete Schechter (1976) function to the data. Instead we fit the low-end slope ($15.5 < m_{UV} < 18$) with an exponential form of slope km_{UV} where m_{UV} is the UV magnitude and k is related to the α parameter of the Schechter function by:

$$\alpha = -(k/0.4 + 1)$$

The resulting UV luminosity function of A1367 shows a slope between $k_{lower} = 0.14 \pm 0.08$ and $k_{upper} = 0.42 \pm 0.09$ (equivalent to $\alpha_{lower} = -1.35 \pm 0.20$ and $\alpha_{upper} = -2.05 \pm 0.22$). Similarly, for the UV luminosity function of Coma we find $k_{lower} = 0.14 \pm 0.09$ and $k_{upper} = 0.37 \pm 0.09$ (equivalent to $\alpha_{lower} = -1.35 \pm 0.22$ and $\alpha_{upper} = -1.94 \pm 0.24$). The upper and lower limits of the UV luminosity functions of the two clusters are in fair agreement, but the allowed range between the two limits is still very broad. Likely the low limit gives a more realistic representation of the true UV luminosity function because nearly all (18/20 or 90%) of the UV selected galaxies for which we obtained a redshift in this work turned out to be in the background. The low limit slope $\alpha \sim -1.35$ is in agreement with the field UV luminosity function of Sullivan et al. (2000) and it is consistent with the slope of the $H\alpha$ luminosity function of the two clusters as determined by Iglesias-Paramo et al. (2002). Certainly the very steep ($\alpha \sim -2.0, -2.2$) luminosity function found for Coma by A99 is due to an underestimate of the density of background galaxies.

6. Summary and conclusions

Optical spectroscopy of 93 galaxies, 60 of which are projected in the direction of Abell 1367, 21 onto the Coma cluster and 12 onto Virgo, is reported. These observations bring the redshift completeness among H α selected galaxies by Iglesias-Paramo et al.(2002) to 100% in the Coma region and to 75% in Abell 1367. All, except one, the H α selected galaxies show H α emission and are confirmed cluster members. The exception is a background galaxy whose [OIII] lines fall in the H α filter. The H α luminosity function of the two clusters determined by Iglesias-Paramo et al. (2002) is fully confirmed.

Redshifts of UV selected galaxies in Coma and A1367 regions were also obtained. With these new data the redshift completeness in the core of the two clusters has reached $\sim 90\%$ for $m_{UV} \leq 16.75$. We re-determine the Coma UV luminosity function and we compute for the first time the UV luminosity function of A1367. The two are found in fair agreement. Their faint-end slopes remain unconstrained ($-2.00 < \alpha < -1.35$) due to the uncertainty on the background counts. However if 90% of the UV selected galaxies without a redshift measurement will be found in the cluster background, as our data indicate, the slope of the UV luminosity function should be near $\alpha \sim -1.35$, in agreement with the field one (Sullivan et al. 2000) and with the H α luminosity functions of the two clusters (Iglesias-Paramo et al. 2002).

Finally we discover a point like H α source in the Virgo cluster, associated with the giant galaxy VCC873, possibly an extragalactic HII region as the one recently observed in Virgo by Gerhard et al.(2002). Objects of this kind could account for the diffuse intracluster light and might contribute to the enrichment of intergalactic medium in galaxy clusters.

Acknowledgements. We wish to thank Jose Donas for providing us with his unpublished catalogue of UV sources in the Coma and Abell 1367 fields. The TACS of the Loiano, Cananea and Calar Alto telescopes are acknowledged for the generous time allocation to this project. This work could not be completed without the NASA/IPAC Extragalactic Database (NED) which is operated by the Jet Propulsion Laboratory, Caltech under contract with NASA.

References

Andreone S., 1999, A&A, 351, 65
 Arnaboldi M., Freeman K. C., Mendez R. H., Capaccioli M., Ciardullo R., Ford H., Gerhard O., Hui X., Jacoby G. H., Kudritzki R. P., Quinn P. J., 1996, ApJ, 472, 145
 Bernstein G. M., Nichol R. C., Tyson J. A., Ulmer M. P., Wittman D., 1995 AJ, 110, 1507
 Binggeli B., Sandage A., & Tammann G., 1985, AJ, 90, 1681
 Boselli A., Iglesias-Paramo J., Vilchez J. M. & Gavazzi G., 2002, A&A, 386, 134
 Deharveng J. M., Boselli A. & Donas J., 2002, A&A, 393, 843
 Dopita M. A., Jacoby G. H., Vassiliadis E., 1992, ApJ, 389, 27

Dopita M. A., Kewley L. J., Heisler C. A., & Sutherland R. S., 2000, ApJ, 542, 224
 Dressler A., 1980, ApJ, 236, 351
 Gerhard, O., Arnaboldi M., Freeman K. C., Okamura S., 2002, ApJ, 580, L121
 Iglesias-Paramo J., Boselli A., Cortese L., Vilchez J.M. & Gavazzi G., 2002, A&A, 384, 383
 Iglesias-Paramo J., Boselli A., Gavazzi G., Cortese L. & Vilchez J.M., 2003, A&A, 397, 421
 Milliard B., Donas J., Laget M., Armand C. & Vuillemin A., 1992, A&A, 257, 24
 Donas, J., Milliard, B. & Laget, M., 1995, A&A, 303, 661
 Theuns T., Warren S., 1997, MNRAS, 284, L11
 Tonry J., Davis M., 1979, AJ, 84, 1511
 Schechter P., 1976, ApJ, 203, 297
 Sullivan M., Treyer M. A., Ellis R. S., Bridges T. J., Milliard B., Donas J., 2000, MNRAS, 312, 442
 Young C. K., Currie M. J., 1998, A&AS, 127, 367

Table 2: Spectroscopic parameters of the observed galaxies.

Name	R.A. (J.2000)	Dec. (J.2000)	r' mag	vel km s ⁻¹	\pm	Lines	Tel.	Sel.
A1367								
114038+195437	11 40 38.96	+19 54 37.4	17.48	7784	96	E	LOI	H α
114110+201117	11 41 10.47	+20 11 17.7	17.57	6952	22	E	LOI	H α
114117+200832	11 41 17.60	+20 08 32.0	15.93	14500	20	E	LOI	UV
114137+194451	11 41 37.90	+19 44 51.0	17.14	27891	80	A	CAN	UV
114141+200230	11 41 41.20	+20 02 30.5	17.37	8447	51	E	LOI	H α
114142+200054	11 41 42.57	+20 00 54.9	17.33	8456	69	E	LOI	H α
114149+194605	11 41 49.79	+19 46 05.1	17.52	7789	39	E	LOI	H α
114156+194836	11 41 57.03	+19 48 36.2	16.53	28896	140	A	CAN	r'
114229+195238	11 42 29.00	+19 52 38.0	17.37	14084	130	A	CAN	UV
114238+192103	11 42 38.40	+19 21 03.0	17.16	18674	72	E	LOI	UV
114240+195716	11 42 40.36	+19 57 16.6	17.68	7501	46	E	LOI	H α
114252+192543	11 42 52.22	+19 25 43.4	15.13	24452	114	A	LOI	r'
114253+201039	11 42 53.11	+20 10 39.8	15.43	6261	192	A	CAN	r'
114300+201225	11 43 00.30	+20 12 25.9	14.90	20965	133	A	CAN	r'
114306+195620	11 43 06.31	+19 56 20.0	15.21	6321	103	A	LOI	r'
114308+194155	11 43 08.00	+19 41 55.0	16.45	12988	16	E	LOI	UV
114311+200144	11 43 11.19	+20 01 44.9	15.37	6994	102	A	CAN	r'
114312+193841	11 43 12.68	+19 38 41.0	16.23	27884	152	A	CAN	r'
114313+193645	11 43 13.08	+19 36 45.8	17.27	6121	131	E	LOI	H α
114314+194016	11 43 14.23	+19 40 16.7	15.03	28078	142	A	CAN	r'
114315+195614	11 43 15.57	+19 56 15.3	16.57	28847	117	A	CAN	r'
114331+200058	11 43 31.30	+20 00 58.0	16.44	30164	23	E	LOI	UV
114337+191836	11 43 37.70	+19 18 36.0	16.65	24154	132	E	CAN	UV
114341+200135	11 43 41.62	+20 01 35.3	17.08	6455	66	E	LOI	H α
114345+192332	11 43 45.41	+19 23 32.0	15.60	27889	258	A	LOI	r'
114350+192606	11 43 50.85	+19 26 06.2	15.31	6135	141	A	CAN	r'
114353+194321	11 43 53.88	+19 43 21.3	17.15	24613	185	A	CAN	r'
114353+194428	11 43 53.77	+19 44 28.6	15.30	6120	131	A	CAN	r'
114355+192743	11 43 55.71	+19 27 43.9	18.72	6427	50	E	LOI	H α
114357+195607	11 43 57.46	+19 56 07.6	15.47	7057	88	A	CAN	r'
114401+191555	11 44 01.10	+19 15 55.0	16.57	28353	76	A	CAN	UV
114401+191707	11 44 01.00	+19 17 07.0	16.92	12784	91	E	CAN	UV
114401+192953	11 44 01.00	+19 29 53.0	16.31	19367	25	E	LOI	UV
114403+194433	11 44 03.31	+19 44 33.0	15.53	6715	101	A	CAN	r'
114407+193724	11 44 07.80	+19 37 24.0	17.28	39774	85	A	CAN	UV
114413+192012	11 44 13.80	+19 20 12.0	16.90	5852	47	E	LOI	r'
114419+191902	11 44 19.30	+19 19 02.0	16.90	26091	217	E	CAN	UV
114430+195718	11 44 30.41	+19 57 18.8	20.23	96341	19	E	LOI	H α
114444+194814	11 44 44.28	+19 48 14.0	19.62	8098	62	E	CAL	H α
114446+194737	11 44 46.13	+19 47 37.5	19.35	8240	59	E	CAL	H α
114446+194639	11 44 46.68	+19 46 39.5	22.03	8383	36	E	CAL	H α
114447+194648	11 44 47.54	+19 46 48.8	21.81	8428	33	E	CAL	H α
114450+194605	11 44 50.81	+19 46 05.1	20.16	8089	50	E	LOI	H α
114451+194717	11 44 51.27	+19 47 17.5	19.24	8022	35	E	LOI	H α
114454+194733	11 44 54.22	+19 47 33.2	18.32	8067	31	E	LOI	H α
114454+200101	11 44 54.55	+20 01 02.0	16.14	7646	500	E	CAN	H α
114459+194757	11 44 59.35	+19 47 57.1	18.42	39550	79	E	LOI	r'
114501+194550	11 45 01.90	+19 45 50.0	16.74	20575	30	E	CAN	UV
114502+194520	11 45 02.71	+19 45 20.6	16.74	20626	13	E	LOI	r'
114505+194514	11 45 05.67	+19 45 14.8	18.07	20263	150	A	CAN	r'
114506+194733	11 45 05.98	+19 47 33.6	16.82	19919	58	E	LOI	r'
114506+200921	11 45 06.56	+20 09 21.4	15.36	6145	184	A	LOI	r'

114513+194523	11 45 13.77	+19 45 22.2	15.84	8316	224	E	CAN	H α	
114514+200836	11 45 14.10	+20 08 36.0	16.99	3752	43	E	CAN	UV	
114518+200009	11 45 18.00	+20 00 09.5	17.54	5327	28	E	LOI	H α	
114525+194905	11 45 25.56	+19 49 05.7	15.22	8422	123	A	CAN	r'	
114541+194613	11 45 41.16	+19 46 13.4	14.89	5419	138	A	CAN	r'	
114545+194130	11 45 45.20	+19 41 30.0	16.48	6123	17	E	CAN	UV	
114558+194810	11 45 58.59	+19 48 10.9	15.41	5493	173	A	LOI	r'	
114611+195110	11 46 11.99	+19 51 10.0	15.07	5441	101	A	CAN	r'	
Coma									
125802+282722	12 58 02.10	+28 27 22.0	17.01	48300	150	A	CAN	UV	
125815+283117	12 58 15.12	+28 31 17.2	16.70	6725	56	E	LOI	UV	
125823+281945	12 58 23.66	+28 19 45.6	16.26	8352	126	A	CAN	r'	
125828+283135	12 58 28.45	+28 31 35.9	15.24	18290	104	A	CAN	r'	
125829+281806	12 58 29.44	+28 18 06.3	15.52	6082	99	A	CAN	r'	
125845+283235	12 58 45.80	+28 32 35.3	17.76	6333	14	E	LOI	H α	
125845+284133	12 58 45.64	+28 41 33.1	17.21	6682	149	E	LOI	H α	
125856+282749	12 58 56.19	+28 27 49.0	15.23	5927	156	A	CAN	r'	
125918+283726	12 59 17.90	+28 37 26.0	16.81	10340	32	E	CAN	UV	
125923+282918	12 59 23.06	+28 29 18.4	15.51	7015	165	E	CAN	H α	
125924+282050	12 59 24.11	+28 20 50.1	16.62	20241	26	E	LOI	UV	
125941+283026	12 59 41.12	+28 30 26.6	15.45	8314	161	A	CAN	r'	
125956+275548	12 59 56.68	+27 55 48.2	15.31	7653	93	A	CAN	r'	
130004+283614	13 00 04.51	+28 36 14.1	15.32	6727	153	A	CAN	r'	
130037+283951	13 00 37.22	+28 39 51.7	16.62	7095	87	E	CAN	H α	
130127+281053	13 01 27.29	+28 10 53.9	17.18	48821	100	A	CAN	r'	
130128+281515	13 01 28.63	+28 15 15.9	20.41	9061	33	E	LOI	H α	
130130+283328	13 01 30.85	+28 33 28.0	16.76	6885	194	E	LOI	H α	
130140+281456	13 01 40.97	+28 14 56.6	19.33	9286	20	E	LOI	H α	
130151+280822	13 01 51.90	+28 08 22.0	17.00	28754	27	A	CAL	UV	
130158+282114	13 01 58.43	+28 21 14.8	19.81	8577	18	E	LOI	H α	
Virgo									
VCC1715	12 37 28.45	+08 47 39.2	15.37	888	32	E	LOI	H α	
VCC 404	12 20 17.50	+04 12 10.0	14.20	1746	93	E	LOI	H α	
VPC766	12 30 46.20	+12 05 57.1	17.05	1162	47	E	LOI	H α	
122544+130740	12 25 44.20	+13 07 40.0	20.10	796	37	E	CAL	H α	
122603+130723	12 26 02.91	+13 07 23.7	21.50	260	34	E	LOI	H α	
122605+130725	12 26 05.75	+13 07 25.7	17.14	23980	40	E	LOI	r'	
123015+122812	12 30 15.20	+12 28 12.0	21.10	79521	37	E	CAL	H α	
123021+121614	12 30 21.10	+12 16 14.0	20.70	90792	36	E	CAL	H α	
123222+090944	12 32 22.81	+09 09 44.1	17.97	77812	50	E	LOI	H α	
123315+091448	12 33 15.25	+09 14 48.0	17.59	30923	29	E	LOI	r'	
123728+082540	12 37 28.00	+08 25 40.0	20.60	79521	33	E	CAL	H α	
124547+102620	12 45 47.32	+10 26 20.5	16.41	36946	144	E	LOI	r'	